The Electronically Excited States of RDX (hexahydro-1,3,5-trinitro-1,3,5-triazine): Vertical Excitations

ITAMAR BORGES JR.,[1] ADÉLIA J. A. AQUINO,[2] MARIO BARBATTI,[2] HANS LISCHKA[2]

[1]*Departamento de Química, Instituto Militar de Engenharia, Praça General Tibúrcio, 80, 22290-270 Rio de Janeiro, Brazil*

[2]*Institute for Theoretical Chemistry, University of Vienna, Währingerstrasse 17, A-1090 Wien, Austria*

Received 19 October 2008; accepted 5 December 2008
Published online 14 April 2009 in Wiley InterScience (www.interscience.wiley.com).
DOI 10.1002/qua.22043

ABSTRACT: The RDX molecule, hexahydro-1,3,5-trinitro-1,3,5-triazine, is a key component for several energetic materials, which have important practical applications as explosives. A systematic study of the electronic excited states of RDX in gas phase using time-dependent density functional theory (TDDFT), algebraic diagrammatic construction through second order method [ADC (2)], and resolution of the identity coupled-cluster singles and doubles method (RI-CC2) was carried out. Transition energies and optical oscillator strengths were computed for a maximum of 40 transitions. RI-CC2 and ADC (2) predict a spectrum shaped by three intense π-π^* transitions, two with charge transfer and one with localized character. TDDFT fails in the description of the charge transfer states. The low-energy band of the experimental UV spectrum of RDX is assigned to the first charge transfer state. Two alternative assignments of the high-energy band are proposed. Int J Quantum Chem 109: 2348–2355, 2009

Key words: RDX; hexahydro-1,3,5-trinitro-1,3,5-triazine; RI-CC2 wave function; TDDFT; excited states; UV spectrum; gas-phase; energetic materials

Correspondence to: I. Borges; e-mail: itamar@ime.eb.br or H. Lischka; e-mail: hans.lischka@univie.ac.at

Contract grant sponsor: The Austrian Science Fund [within the framework of the Special Research Program F16 (Advanced Light Sources) and project P18411-N19].

Contract grant sponsor: CNPq and CAPES, Brazilian agencies.

Additional Supporting Information may be found in the online version of this article.

Introduction

Energetic materials are subject to complicated physical-chemical processes because they combine several phases, multiple reactions, and excited states [1]. Among these processes, electronic excitation has been experimentally verified to play an important role in the initiation of the detonation of energetic materials [2]. In particular, gas phase investigations of these materials may provide insights on the properties and reactions at the molecular level and allow for detailed studies with respect to their decomposition, especially under consideration of their excited states.

Energetic materials such as hexahydro-1,3,5-trinitro-1,3,5-triazine, known as RDX, have important practical applications ranging from automobile air bags to rocket propellants. Gas-phase RDX is a relatively stable molecule, which contains three NO_2 groups and releases a large amount of energy upon decomposition [3]. This molecule belongs to the class of nitramines with general formula $RR'N(NO_2)$. Like most of the compounds containing NO_2 groups, RDX has a diffuse electronic spectrum, a tendency to dissociation and shows a variety of associated photochemical phenomena [4]. In particular, it is known that UV excitation markedly reduces the power requirements for detonation of secondary explosives [5]. Moreover, since nitro-organic compounds show strong ultraviolet (UV) absorption, the knowledge and understanding of their electronic excitation spectrum can also help in the design of explosive detectors. In particular, direct detection of nitro-organic explosives can be achieved through the coupling of gas-phase UV absorption with gas chromatography techniques [6].

Because of a wide range of practical applications, RDX has been studied extensively both theoretically and experimentally [2, 7]. Solid and gas-phase properties have been experimentally investigated by means of mass spectroscopy, femtosecond pump-probe spectroscopy [2], and measurements of the UV spectrum [8]. Theoretical studies, on their turn, have focused on ground states properties such as energetic conformations [9], vibrational spectra [10], and unimolecular dissociation [11]. Concerning theoretical calculations on excited states of RDX, we are aware of the semiempirical complete neglect of differential overlap (CNDO) based work of Orloff et al. [8] and the ab initio restricted configuration interaction with single excitation (RCIS/6-31+G) investigation of Bernstein and coworkers [2]. The former investigators computed the first six RDX vertical singlet transitions, their character, and oscillator strengths, whereas the latter aimed at the geometry optimization of the first excited singlet state but could only report the first excited state transition energy. The CNDO results [8], obtained in the 5.7–6.5 eV energy range, predicted the existence of two bands, both assigned to $\pi \rightarrow \pi^*$ transitions.

It is the purpose of this work to present calculations on the UV spectrum of RDX based on current state-of-the-art methods available for molecules of the size of RDX. These investigations should provide the first step into a better understanding of the dissociation dynamics of RDX [2]. The methods used include the approximate singles-and-doubles approach using the resolution of the identity coupled-cluster (RI-CC2) [12, 13], the algebraic diagrammatic construction through second order method [ADC(2)] [14, 15], and the time-dependent density functional theory (TDDFT) [16, 17]. In particular, because of its computational efficiency the TDDFT method is very attractive but may be subject to various artifacts, such as those related to the description of charge-transfer states [18]. The RI-CC2 and the ADC(2) calculation have been additionally employed to assess the performance of TDDFT. Vertical transition energies and optical oscillator strengths were computed for a maximum of 40 transitions.

Computational Details

In the ground state, the RDX molecule possesses C_{3v} symmetry [19]. Two possible geometries known as AAA and EEE structures have been found, where an A represents an NO_2 group in the axial position and an E in the equatorial position. The AAA structure is shown in Figure 1. Since the lowest energy and most probable experimental structure is the AAA form [9, 19], we optimized this structure at the B3LYP/6-31G(d,p) level and using a series of basis sets (split-valence polarized (SVP) [20], triple-zeta valence polarized (TZVP) [21], TZVPP [22], and TZVPP′) for the RI-CC2 approach. The prime in TZVPP′ indicates that the f functions were removed from the heavy atoms and the d function from the hydrogen atoms. Frequency calculations confirmed the minimum energy character.

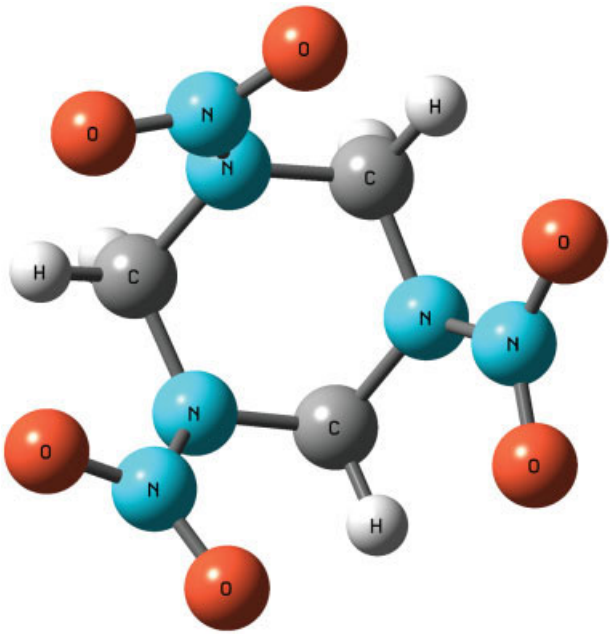

FIGURE 1. Molecular structure of RDX. [Color figure can be viewed in the online issue, which is available at www.interscience.wiley.com.]

The RI-CC2, ADC(2), and TDDFT/B3LYP methods were employed for the calculation of vertical excited states using the RI-CC2/TZVPP ground-state geometry. The core orbitals (first nine a′ and six a″ orbitals) were frozen in the RI-CC2 and ADC(2) calculations. The SVP and the TZVP basis sets were used for all three methods. Polarization effects were also tested by means of the TZVPP′ basis set. At TDDFT level only, the vertical excitations were additionally computed with the TZVP basis sets increased by a set of diffuse p functions (TZVP+p) and with the aug-cc-pVTZ basis set [23]. The calculations were performed using the Turbomole suite of programs employing C_s symmetry. Estimation of solvent effects on the transition energies were performed at the TDDFT/B3LYP level with the PCM model [24]. The DFT calculations were performed using the Gaussian03 [25, 26] program. The TDDFT and RI-CC2 calculations were performed with the Turbomole program) [27].

Results and Discussion

In Figure 1, the RDX structure is presented. Table I shows selected geometric parameters computed with the RI-CC2 method using the sequence of SVP, TZVP, TZVPP′, and TZVPP basis sets and a comparison with results obtained with the B3LYP/6-31G(d,p) method. B3LYP/6-31G(d) geometry optimizations have been performed before by Vladimiroff and Rice [9]. The present B3LYP/6-31G(d,p) geometry data agree well with their finding. It was the purpose of the present RI-CC2 calculations using extended basis sets to establish first of all a benchmark ground-state geometry for RDX.

Comparing bond distances in Table I, it is seen that the N—N bond is most sensitive. Variations are found at the RI-CC2 level using different basis sets within the range of 0.02 Å. It appears that the inclusion of f functions is important. Interestingly, the N—N bond distance computed with the TZVPP basis comes close to the SVP result. The difference to the B3LYP/6-31G(d,p) results is significant amounting to 0.024 Å for RI-CC2/TZVPP. Other

TABLE I

RDX geometrical parameters: B3LYP/6-31G(d,p) and RI-CC2 results the latter obtained with different basis sets.

Geometrical parameter	B3LYP/6-31G(d,p)	CC2/SVP	CC2/TZVP	CC2/TZVPP′	CC2/TZVPP
C—N	1.460	1.453	1.458	1.458	1.454
N—N	1.422	1.440	1.464	1.458	1.446
N═O	1.222	1.230	1.237	1.237	1.232
C—H	1.086	1.094	1.085	1.083	1.084
NCN	112.7	113.1	114.7	114.4	114.0
CNN	117.4	116.5	115.3	115.3	115.8
ONO	127.0	127.8	128.0	127.9	127.9
HCN	109.7	109.6	109.6	109.5	109.5

Distances are given in Å and angles in degrees (°).

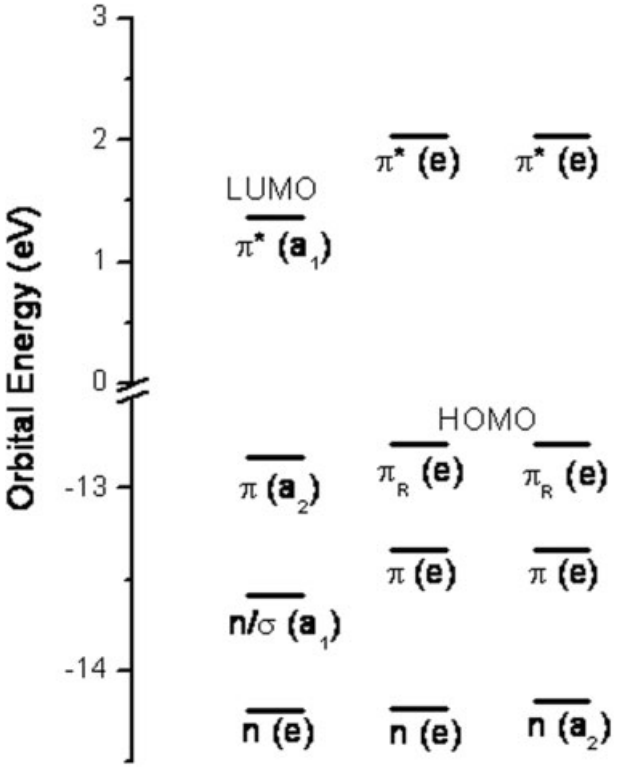

FIGURE 2. Orbital energy diagram of the most important SCF/TZVP orbitals for RDX. The character of each orbital is shown with the corresponding notation in C_{3v} symmetry in parentheses.

relevant discrepancies are observed for the N═O distances with the B3LYP/6-31G(d,p) and RI-CC2/TZPP methods (0.010 Å) and for the N—H separation obtained with the RI-CC2/SVP and RI-CC2/TZVPP approaches (0.012 Å). The largest difference between angles equals 1.6° for NCN using the B3LYP/6-31G(d,p) and RI-CC2/TZVPP methods. The remaining RDX distances and angles have smaller differences. The RI-CC2/TZVPP geometry was used for all the vertical calculations.

In Figure 2, the orbital energy diagram for the SCF/TZVP molecular orbitals is given. The most relevant orbitals in the present context have lone pair character on the oxygen atoms (n), π character mostly localized on the NO_2 moieties, and π character mostly localized in the ring nitrogen atoms (π_R). These orbitals, computed at SCF/TZVP level, are displayed in Figure 3. The B3LYP/TZVP orbitals are collected in the Supporting information for comparison. The n and π orbitals are defined with respect to the plane containing a NO_2 group. This orbital pattern characterizing the valence transitions in RDX is typical of molecules having a NO_2 group. A similar picture has been found in our previous investigations on dimethylnitramine [28] and nitramide [29]. Both molecules have an NO_2 group, although for these systems the set of relevant valence orbitals for the calculated transitions includes more n orbitals than in the RDX molecule. One of the n orbitals shows a strong mixing with a σ orbital along the NN bond. The excited states discussed below can be characterized in terms of single excitations from the nine valence orbitals into the three π^* orbitals displayed in Figures 2 and 3. This set of 12 orbitals is grouped into subsets of three, with the orbitals within each group having a pair of degenerate orbitals and the remaining one being close in energy, which reflects the C_{3v} point group symmetry. In particular, this pattern of the highest occupied orbitals determines the appearance of quasi-triply degenerate transitions, with the degenerate pair naturally having the same optical oscillator strengths and the remaining one in most cases having quite different values.

Twenty vertical singlet transitions, 10 for each irreducible representation in C_s symmetry, were com-

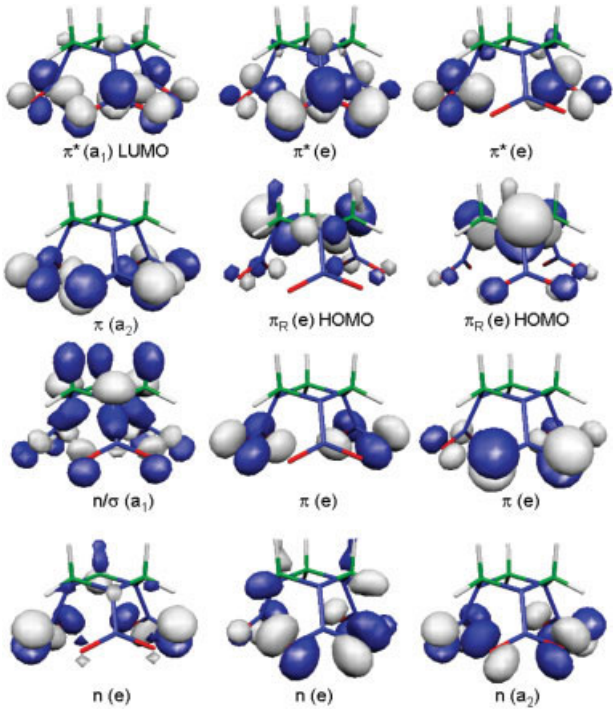

FIGURE 3. RDX SCF/TZVP molecular orbitals ordered according to the orbital scheme given in Figure 2. [Color figure can be viewed in the online issue, which is available at www.interscience.wiley.com.]

TABLE II

Basis set dependence of the RI-CC2, ADC(2), and TDDFT(B3LYP) methods for selected electronic transitions.

Method	Basis set	ΔE (eV) π_R-π^*	n-π^*	π-π^*
RI-CC2	SVP	5.44	6.27	7.32
	TZVP	5.27	6.04	6.98
	TZVPP′	5.24	6.01	6.97
ADC(2)	SVP	6.24	5.17	6.79
	TZVP	5.98	5.02	6.46
	TZVPP′	5.95	5.02	6.46
TDDFT (B3LYP)	SVP	5.46	5.90	7.79
	TZVP	5.55	5.79	7.31
	TZVPP′	5.32	5.80	7.30
	TZVP+p	4.58	5.38	6.90
	aug-cc-pVTZ	4.62	5.40	7.19

puted with the RI-CC2 and ADC(2) methods. Forty transitions were calculated at the TDDFT(B3LYP) level. A wide range of basis sets extending up to TZVPP′ quality was used for the three approaches. First, the basis set effects on the RI-CC2, ADC(2), and TDDFT results are considered. Table II shows the basis set dependence of the three methods for a set of three transitions selected by their importance for the composition of the RDX UV spectrum. The complete set of electronic transitions computed with the different basis set can be seen in the Tables of the Supporting information. As expected, the main effect is the stabilization of the excited states when increasing the basis set from the SVP to TZVP. Low-energy transitions show smaller basis set dependence ranging in the order of 0.1 eV, whereas higher energy transitions are more sensitive to the basis set with energy changes of up to 0.9 eV. The extension of polarization functions when moving from TZVP to TZVPP′ affects the results only to a small extent. In the case of TDDFT, the vertical excitation energies were computed also with the TZVP+p and the aug-cc-pVTZ. For the former, a quite significant stabilization of the π-π^* state was found. Overall, the TDDFT method seems less sensitive to basis set effects than the other two methods.

Complete RI-CC2, ADC(2), and TDDFT results for transition energies and optical oscillator strengths computed with the TZVPP′ basis set are given in Tables III and IV. In these Tables, the transitions are given according to the C_{3v} labeling. For the three methods, the first excited state is the dark $1A_2$ state corresponding to an n-π^* transition. The first bright transition at RI-CC2 and TDDFT levels leads into the 2E state, corresponding to the charge transfer (CT) π_R-π^* state. In this transition, one electron located in the π_R orbital at the ring nitrogen atoms is transferred to the π^* orbital at the NO_2 group. The state has also contribution from a σ_{NN}-π^* configuration, which indicates that the ac-

TABLE III

Computed transition energies (ΔE) and oscillator strengths (f) for RDX based on the RI-CC2/TZVPP′ and ADC(2)/TZVPP′ approaches.

RI-CC2/TZVPP′			ADC(2)/TZVPP′		
State	ΔE (eV)	f	State	ΔE (eV)	f
$1A_2$	4.50	0.000	$1A_2$	4.18	0.000
1E	4.54	0.000	1E	4.22	0.000
2E	5.24	0.064	2E	5.02	0.026
$1A_1$	5.36	0.025	$1A_1$	5.06	0.014
3E	5.63	0.041	3E	5.51	0.066
$2A_1$	6.01	0.126	$2A_1$	5.95	0.150
4E	6.59	0.000	$2A_2$	6.09	0.000
$2A_2$	6.59	0.000	4E	6.46	0.611
$3A_2$	6.78	0.000	5E	6.63	0.052
5E	6.97	0.473	$3A_2$	6.82	0.000
$4A_2$	7.35	0.002	$4A_2$	7.20	0.000
6E	7.35	0.006	6E	7.21	0.003
$3A_1$	7.40	0.001	$3A_1$	7.34	0.002
$4A_1$	7.64	0.001	$4A_1$	7.68	0.001

TABLE IV

Computed transition energies (ΔE) and oscillator strengths (f) for RDX based on the TDDFT(B3LYP)/TZVPP′ approach.

State	ΔE (eV)	f	State	ΔE (eV)	f
$1A_2$	4.64	0.000	7E	6.35	0.050
1E	4.64	0.002	8E	6.43	0.004
2E	5.32	0.077	9E	6.61	0.012
$1A_1$	5.43	0.006	$5A_1$	6.72	0.001
3E	5.54	0.000	10E	6.82	0.020
$2A_2$	5.62	0.000	$5A_2$	6.97	0.000
4E	5.66	0.030	$6A_2$	7.22	0.000
$2A_1$	5.80	0.048	11E	7.30	0.227
$3A_2$	5.91	0.002	$6A_1$	7.38	0.027
5E	5.92	0.018	12E	7.44	0.077
$4A_2$	6.13	0.009	13E	7.66	0.002
$3A_1$	6.14	0.010	$7A_2$	7.94	0.000
6E	6.27	0.017	$7A_1$	8.09	0.029
$4A_1$	6.30	0.044			

tivation of this state may lead to NO_2 fragmentation. This is consistent with the dissociative character of the CT state in nitramide along the NH_2+NO_2 channel computed with the CASPT2 method [30]. The first bright transition at ADC(2) level is also into the 2E state, but in this case, it corresponds to an n-π^* excitation.

Despite a slightly different order, RI-CC2 and ADC(2) methods predict a similar sequence of n-π^* and π-π^* bright states. In both cases, the spectrum is dominated by three intense transitions. The first two of these transitions—2E and $2A_1$ for RI-CC2 and 3E and $2A_1$ for ADC(2)—are CT π_R-π^* states. The third one—5E in the case of RI-CC2 and 4E in the case of ADC(2)—is a localized π-π^* excitation (LE) involving orbitals centered at the NO_2 groups. In the case of TDDFT, the CT π_R-π states (2E and 4E) have low intensities, which are comparable to the intensities of the n-π^* transitions. These states have also too low energies in comparison to the RI-CC2 and ADC(2) results, which is a strong indication that the TDDFT method shows the well-known artifacts in the prediction of CT states [18]. It is planned to use newly developed DFT functionals designed to deal with CT states [31, 32] in future investigations for better description of these states in RDX. As expected, the TDDFT description of the third intense transition, the LE π-π^* (11E) state is in good agreement with the RI-CC2 and ADC(2) predictions.

To estimate the solvent effect on the transitions energies, TDDFT(B3LYP) transition energies were calculated both in vacuum and in acetonitrile, the latter using the PCM model [24]. Twenty states were investigated. The largest difference between the transition energies in vacuum and in acetonitrile was a blue shift of 0.15 eV. Nevertheless, we should take into account that investigations of the solvent effects on CASPT2 calculations for nitramide [30] have shown strong effects on the CT state for a broad range of solvents. Again, this indicates the poor description of these states in the TDDFT/B3LYP approach.

The experimental RDX UV spectrum in acetonitrile has two distinct maxima at 5.25 eV and at 6.34 eV, the latter being most intense [8]. This spectrum is shown in Figure 4 along with our RI-CC2/TZVPP′ and TDDFT/TZVPP′ vacuum results. The spectrum of dimethylnitramine $[(CH_3)_2NNO_2]$ [33] in gas phase is very similar, with two bands at 5.4 eV and 6.4 eV. In nitramide $[H_2NNO_2]$ measured in different solvents, only one broad band was observed [34]. The authors of this study claimed that

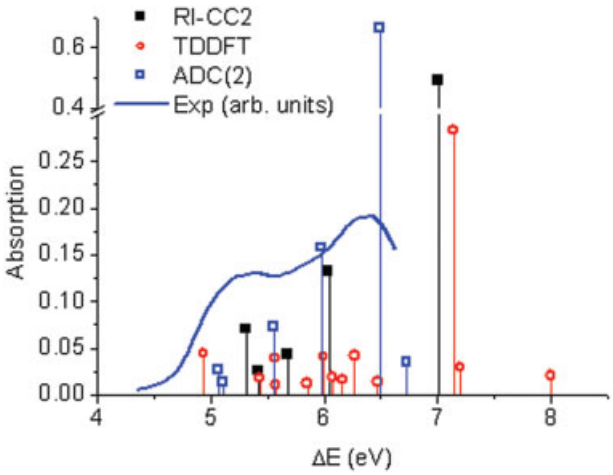

FIGURE 4. Computed RI-CC2/TZVP, ADC(2) and TD-DFT/TZVP spectra in comparison with the experimental UV spectrum in acetonitrile [8]. The label *f* indicates the computed oscillator strengths while the full line represents the experimental spectrum. Only states with $f \geq 0.01$ are shown. [Color figure can be viewed in the online issue, which is available at www.interscience.wiley.com.]

this unique band was formed by the superposition of CT and NO_2-localized π-π^* transitions. Our current calculations at RI-CC2 and ADC(2) levels show that the low energy band of RDX is due to the CT π_R-π^* state. The broadness of this band can partially be attributed to the dissociative character of this state mentioned above. Besides that, the sequence of low intensity n-π^* transitions should also contribute to the final broadening (Table V).

The assignment of the second band is, however, not so clear and our results allow for two different possibilities. Firstly, the second band can be assigned to the second CT π_R-π^* state. This is the assignment indicated in Table V. In this case, the transition energy of the second CT π_R-π^* state computed either with RI-CC2 or ADC(2) is too low by about 0.4–0.5 eV in comparison to the experimental data. This difference could be in principle explained by solvent effects. One important consequence of this assignment is that it implies that the most intense absorption band of RDX has not been measured so far. It should correspond to the LE π-π^* transition around 6.97 eV (178 nm) according to the RI-CC2/TZVPP′ level, which opens the possibility of experimental verification of this assignment.

Alternatively, the high energy band can be assigned to the LE π-π^* transition. In this case, the second π_R-π^* state would be one more state con-

TABLE V

Assignment of the experimental bands in the UV spectrum of RDX.

RI-CC2/TZVPP′				ADC(2)/TZVPP′				TDDFT(B3LYP)/TZVPP′				Exp.
State	ΔE (eV)	f		State	ΔE (eV)	f		State	ΔE (eV)	f		ΔE (eV)
2E	5.24	0.064	π_R-π^*	2E	5.02	0.026	n-π^*	2E	5.32	0.077	π_R-π^*	5.25[a]
$1A_1$	5.36	0.025	n-π^*	$1A_1$	5.06	0.014	n-π^*	4E	5.66	0.030	π_R-π^*	(5.4)[b]
3E	5.63	0.041	n-π^*	3E	5.51	0.066	π_R-π^*	$2A_1$	5.80	0.048	n-π^*	
$2A_1$	6.01	0.126	π_R-π^*	$2A_1$	5.95	0.150	π_R-π^*	6E	6.27	0.017	n-π^*	6.34[a]
								$3A_1$	6.14	0.010	n-π^*	(6.4)[b]
								7E	6.35	0.050	π-π^*	
								9E	6.61	0.012	π-π^*	
5E	6.97	0.473	π-π^*	4E	6.46	0.606	π-π^*	11E	7.30	0.227	π-π^*	
				5E	6.63	0.064	π_R-π^*	$6A_1$	7.38	0.027	π-π^*	

[a] RDX in acetonitrile. Experimental data from Ref. [8] (band maximum).
[b] Dimethylnitramine in gas phase. Experimental data from Ref. [32] (band maximum).

tributing to the first band and to the region of overlap. The ADC(2) result is particularly in agreement with this hypothesis, since it predicts the LE π-π^* state at 6.46 eV. The RI-CC2 and TDDFT transition energies, however, are, respectively, 6.97 and 7.30 eV, clearly too high by at least 0.5 eV to support this assignment.

Conclusions

The excited electronic states of the RDX molecule in gas phase were studied with the RI-CC2, ADC(2), and TDDFT methods using a sequence of double-ζ and triple-ζ quality basis sets. Vertical transition energies and optical oscillator strengths were obtained for a maximum of 40 states at each level. Extended geometry optimizations in the ground state have been performed using the RI-CC2 method. The present calculations constitute the most accurate benchmark of excitation energies for RDX so far.

Both RI-CC2 and TDDFT results show quasi-triply degenerate excitations. The RI-CC2 and ADC(2) methods predict that the UV spectrum is dominated by three specially bright transitions associated with excitations to two charge transfer states and one localized π-π^* state. The TDDFT results are in agreement with RI-CC2 and ADC(2) only in case of the highest energy transition and fails in its description of the charge transfer states. The UV spectrum predicted by this method is mostly formed by a sequence of low intensity transitions. The low energy band of the experimental UV spectrum of RDX in acetonitrile is assigned to the first charge transfer state. Two alternative assignments of the high energy band are proposed. In the first one, the band is assigned to the second charge transfer state, whereas in the second possibility the band is assigned to the localized π-π^* state. If the first hypothesis is correct, a strong additional UV band at about 178 nm should exist for RDX.

ACKNOWLEDGMENTS

The authors are grateful for technical support and computer time at the Linux PC cluster Schrödinger III of the computer center of the University of Vienna.

References

1. Shaw, R. W.; Brill, T. B.; Thompson, D. L. Overviews of Recent Research on Energetic Materials; World Scientific: Singapore, 2005.
2. Guo, Y. Q.; Greenfield, M.; Bhattacharya, A.; Bernstein, E. R. J Chem Phys 2007, 127, 154301.
3. Chakraborty, D.; Muller, R. P.; Dasgupta, S.; Goddard, W. A. J Phys Chem A 2000, 104, 2261.
4. Harris, L. E. J Chem Phys 1973, 58, 5615.
5. Im, H. S.; Bernstein, E. R. J Chem Phys 2000, 113, 7911.
6. Hodyss, R.; Beauchamp, J. L. Anal Chem 2005, 77, 3607.
7. Agrawal, P. M.; Rice, B. M.; Zheng, L. Q.; Thompson, D. L. J Phys Chem B 2006, 110, 26185.
8. Orloff, M. K.; Mullen, P. A.; Rauch, F. C. J Phys Chem 1970, 74, 2189.
9. Vladimiroff, T.; Rice, B. M. J Phys Chem A 2002, 106, 10437.

10. Torres, P.; Mercado, L.; Cotte, I.; Hernandez, S. P.; Mina, N.; Santana, A.; Chamberlain, R. T.; Lareau, R.; Castro, M. E. J Phys Chem B 2004, 108, 8799.
11. Guo, Y.; Thompson, D. L.; Miller, W. H. J Phys Chem A 1999, 103, 10308.
12. Kohn, A.; Hattig, C. J Chem Phys 2003, 119, 5021.
13. Hattig, C. J Chem Phys 2003, 118, 7751.
14. Schirmer, J. Phys Rev A 1982, 26, 2395.
15. Trofimov, A. B.; Schirmer, J. J Phys B At Mol Opt Phys 1995, 28, 2299.
16. Furche, F.; Ahlrichs, R. J Chem Phys 2002, 117, 7433.
17. Bauernschmitt, R.; Haser, M.; Treutler, O.; Ahlrichs, R. Chem Phys Lett 1997, 264, 573.
18. Dreuw, A.; Weisman, J. L.; Head-Gordon, M. J Chem Phys 2003, 119, 2943.
19. Karpowicz, R. J.; Brill, T. B. J Phys Chem 1984, 88, 348.
20. Schafer, A.; Horn, H.; Ahlrichs, R. J Chem Phys 1992, 97, 2571.
21. Schafer, A.; Huber, C.; Ahlrichs, R. J Chem Phys 1994, 100, 5829.
22. Weigend, F.; Haser, M.; Patzelt, H.; Ahlrichs, R. Chem Phys Lett 1998, 294, 143.
23. Dunning, T. H. J Chem Phys 1989, 90, 1007.
24. Tomasi, J.; Mennucci, B.; Cammi, R. Chem Rev 2005, 105, 2999.
25. Becke, A. D. J Chem Phys 1993, 98, 5648.
26. Frisch, M. J.; Trucks, G. W.; Schlegel, H. B.; Scuseria, G. E.; Robb, M. A.; Cheeseman, J. R.; Montgomery, J. J. A.; Vreven, T.; Kudin, K. N.; Burant, J. C.; Millam, J. M.; Iyengar, S. S.; Tomasi, J.; Barone, V.; Mennucci, B.; Cossi, M.; Scalmani, G.; Rega, N.; Petersson, G. A.; Nakatsuji, H.; Hada, M.; Ehara, M.; Toyota, K.; Fukuda, R.; Hasegawa, J.; Ishida, M.; Nakajima, T.; Honda, Y.; Kitao, O.; Nakai, H.; Klene, M.; Li, X.; Knox, J. E.; Hratchian, H. P.; Cross, J. B.; Bakken, V.; Adamo, C.; Jaramillo, J.; Gomperts, R.; Stratmann, R. E.; Yazyev, O.; Austin, A. J.; Cammi, R.; Pomelli, C.; Ochterski, J. W.; Ayala, P. Y.; Morokuma, K.; Voth, G. A.; Salvador, P.; Dannenberg, J. J.; Zakrzewski, V. G.; Dapprich, S.; Daniels, A. D.; Strain, M. C.; Farkas, O.; Malick, D. K.; Rabuck, A. D.; Raghavachari, K.; Foresman, J. B.; Ortiz, J. V.; Cui, Q.; Baboul, A. G.; Clifford, S.; Cioslowski, J.; Stefanov, B. B.; Liu, G.; Liashenko, A.; Piskorz, P.; Komaromi, I.; Martin, R. L.; Fox, D. J.; Keith, T.; Al-Laham, M. A.; Peng, C. Y.; Nanayakkara, A.; Challacombe, M.; Gill, P. M. W.; Johnson, B.; Chen, W.; Wong, M. W.; Gonzalez, C.; Pople, J. A. Gaussian 03, Revision C. 02. Gaussian, Inc.: Wallingford, CT, 2004.
27. Ahlrichs, R.; Bar, M.; Haser, M.; Horn, H.; Kolmel, C. Chem Phys Lett 1989, 162, 165.
28. Borges, I. Chem Phys 2008, 349, 256.
29. Borges, I. Theor Chem Acc 2008, 121, 239.
30. Arenas, J. F.; Otero, J. C.; Pelaez, D.; Soto, J. J Phys Chem A 2005, 109, 7172.
31. Peach, M. J. G.; Helgaker, T.; Salek, P.; Keal, T. W.; Lutnaes, O. B.; Tozer, D. J.; Handy, N. C. Phys Chem Chem Phys 2005, 8, 558.
32. Zhao, Y.; Truhlar, D. G. J Phys Chem A 2006, 110, 13126.
33. McQuaid, M. J.; Sausa, R. C. Appl Spectrosc 1991, 45, 916.
34. Kaya, K.; Kuwata, K.; Nagakura, S. Bull Chem Soc Jpn 1964, 37, 1055.